SUBCONTRACT TITLE: Innovative Characterization of Amorphous and Thin-Film Silicon for Improved Module Performance

SUBCONTRACT NO: NREL Subcontract ZXL-5-44205-11

QUARTERLY TECHNICAL STATUS REPORT: Phase II/Quarter 1
28 July 2006 to 27 October 2006

SUBMITTED TO: Bolko von Roedern
National Renewable Energy Laboratory

PRINCIPAL INVESTIGATOR: J. David Cohen, Department of Physics
University of Oregon, Eugene, OR 97403

This report covers the second quarter of Phase II for the period 28 July 2006 to 27 October 2006 of the Thin Film Partnership Subcontract ZXL-5-44205-11. Our Statement of Work calls for us to devote roughly 30% of our effort to CIS thin-film photovoltaics, and 70% to silicon-based thin film technologies. Accordingly, this Quarterly will be devoted to reporting the some of our results obtained studying CIGS cells. The primary results to be reported from work in my laboratory during this period concerns a study to try to better understand the beneficial effects of Na impurities on CIGS device performance.

The addition of Na to the CIGS absorber layer is a commonly followed procedure, boosting the efficiency by up to 50% primarily through a sizeable increase in the open-circuit voltage (V_{oc}) and the fill factor (FF). Although the positive role of Na is well known, there is an ongoing debate as to the exact mechanism of the beneficial effect of Na, with much of the debate centering around where in the cell the Na has its effect. Possible sites are grain boundaries, in the bulk of the grains, or the CdS/CIGS heterojunction. Recent experimental results appear quite contradictory, with one group finding no evidence of Na at the grain boundaries[1] and another group concluding that the Na is only found in significant amounts at the grain boundaries[2]. Another group hypothesizes that the Na acts only during the growth of the sample to organize and passivate point defects[3]; however, this is disputed by similar benefits obtained through diffusion of Na into the sample in a post-deposition treatment[4].

A pair of matched baseline (34017.12) and reduced Na (34017.32) samples were provided to us by the Institute of Energy Conversion in May, 2006. The samples were co-deposited at 550°C in a single deposition with a thickness of 2.0 μm. The baseline film was deposited on a Mo-coated soda lime glass substrate and the reduced Na film was deposited on a substrate provided by Shell Solar which has a SiO_2 diffusion barrier below the Mo. Both devices were completed with standard CdS, ZnO and ITO depositions and a Ni/Al grid. Table I provides the device performance parameters of the cells analyzed and discussed below. These parameters were typical for all of the cells on the samples. The differences between these samples exhibit the

Table I: Device performance parameters of the matched CIGS devices with and with less Na.

Cell	Voc (V)	Jsc (mA)	FF (%)	Eff (%)
34017.12 – 1 (Na)	0.624	32.9	74.0	15.2
34017.32 – 4 (reduced Na)	0.494	33.6	64.3	10.7

commonly known effects of Na on CIGS solar cells: An increased V_{oc}, fill factor, and efficiency (by nearly 50%), with virtually no effect on short circuit current.

Secondary Ion Mass Spectroscopy (SIMS) was performed on a similar pair of samples. These profiles, shown in Fig. 1, indicate a difference in the relative Na density from a factor of five near the back contact to a factor of nearly 100 near the front between the Na and reduced Na samples. Thus, the Na appears to be segregating towards the front of the sample when it is intentionally added.

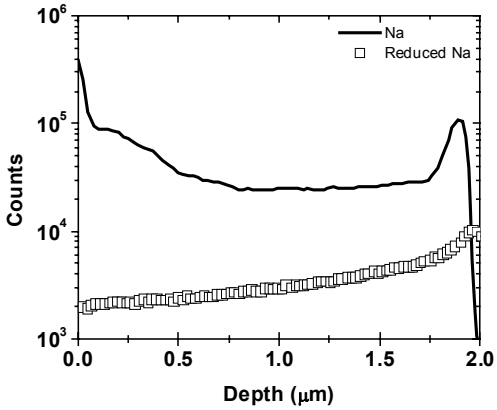

FIG. 1. SIMS depth profiles of a similar pair of higher and lower Na CIGS samples.

Drive-level capacitance profiles are displayed for the CIGS samples with and without Na in Fig. 2. These profiles show similar overall shapes but more spatial variation in the sample with Na. The sample with Na shows a defect activating between 130 K and 190 K that is absent in the reduced Na sample. Without any prior knowledge of cell performance, one would predict that the more spatially uniform, reduced Na sample to be more efficient. Exactly the opposite is the case. Thus, this indicates that something not visible in the DLC profiles is having a dramatically harmful effect on the performance of the low Na cell.

These profiles indicate free carrier densities of 3×10^{14} cm^{-3} for the Na sample and 1.2×10^{14} cm^{-3} for the reduced Na sample. From the higher temperature profiles we infer a deep acceptor density of $\sim1\times10^{15}$ cm^{-3} in the higher Na sample. The reduced Na sample does not show this type of defect, instead it increases only slightly with temperature to a maximum value of $\sim3\times10^{14}$ cm^{-3}. The abrupt increase in the DLC profiles near the junction (<x> = 0) may reflect a significant defect density near the junction, however we are not certain whether the DLCP can provide an accurate measurement of the defect density in this region. We thus choose to use the more spatially uniform region of the profiles to estimate the free carrier and defect densities.

In Fig. 3 we compare the TPC spectra for the Na and reduced Na samples. The spectra have

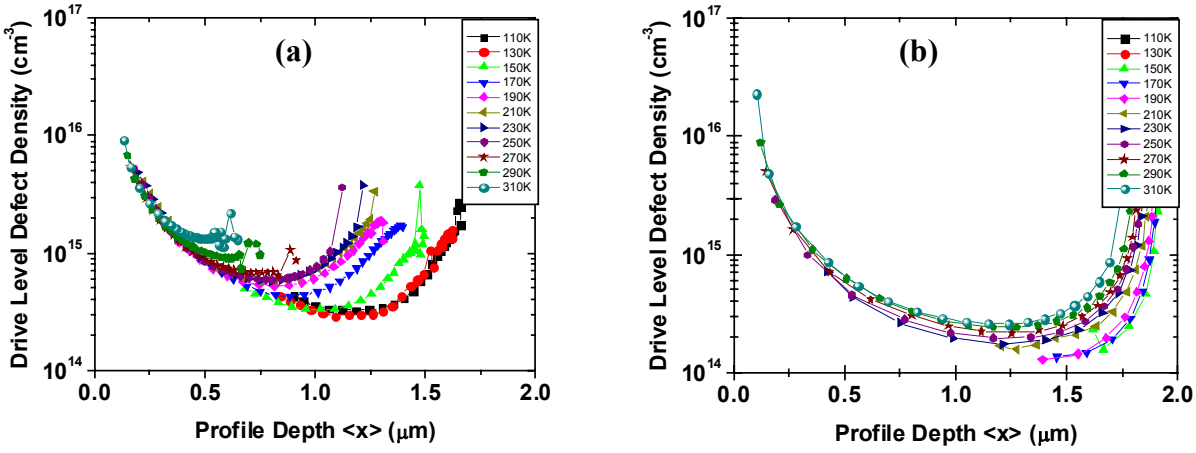

FIG. 2. DLC Profiles for a) Na and b) reduced Na samples. These profiles were obtained at 10 kHz at the temperatures indicated with an applied dc bias ranging from at least 1.0 V reverse to 0.3 V forward. The profiles have similar shapes, and the higher Na sample appears to exhibit a larger deep defect response. However, that cell is 50% more efficient than the reduced Na cell.

been aligned above the 1.2 eV gap energy to enable a better comparison. The spectra are surprisingly similar, and the thin solid lines indicate fits in which we have assumed a gaussian defect band and an exponential band tail. The sample containing Na exhibits an Urbach energy of 17 meV plus a gaussian defect band centered at 0.75 eV above E_V with a FWHM near 120 meV. The Urbach energy for the low Na sample is larger, 23 meV, and the gaussian defect band appears centered at 0.70 eV with a much smaller width, about 50 meV. The narrower bandtail for the sample with Na suggests a higher degree of crystalline order within the CIGS absorber[5].

Admittance spectra were obtained for each of these samples for frequencies between 100 Hz and 100 kHz and temperatures between 80 K and 280 K. With 0 V applied bias, there is a very distinct activated step in the sample with Na, but no such clear feature in the reduced Na sample, as shown in Fig. 4(a) and (b). The step in the Na sample has an

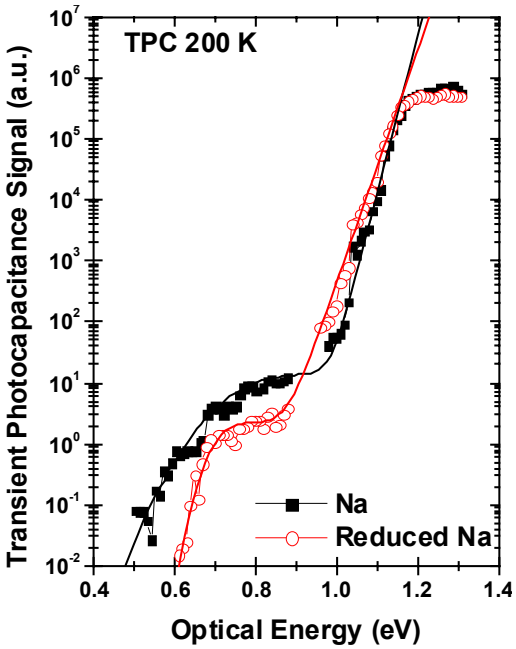

FIG. 3. TPC Spectra of the two samples. The reduced Na sample spectrum exhibits a broader bandtail, indicating a higher level of disorder.

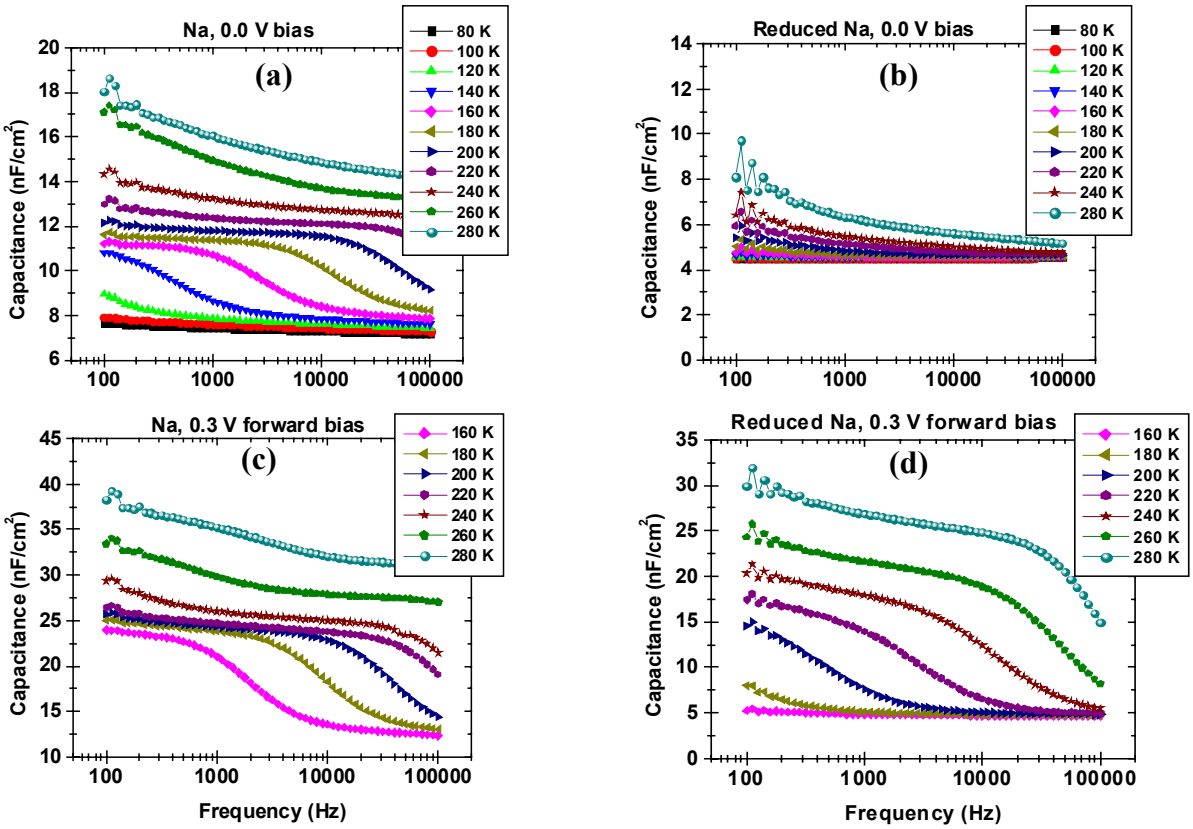

FIG. 4. Admittance spectra for (a) & (c) the Na containing sample, and (b) & (d) the reduced Na sample. The reduced Na sample shows a step only visible under an applied forward bias.

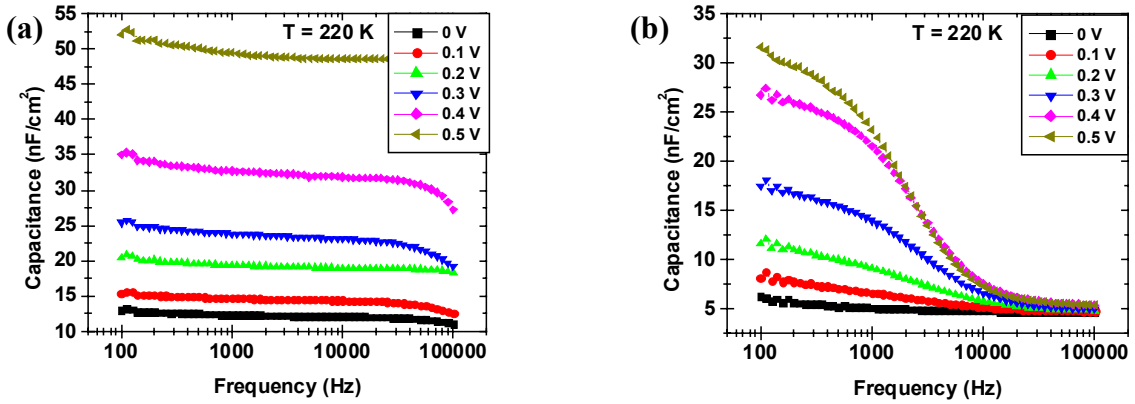

FIG. 5. Admittance vs applied voltage for (a) Na sample, 280 K and (b) reduced Na sample, 220 K. The appearance of the capacitive step under forward bias and the limit in its magnitude for the reduced Na sample are both characteristic responses of an significant interface state.

activation energy of 270 meV as determined by an Arrhenius plot, consistent with many previous admittance measurements of CIGS materials. It is worth pointing out that many researchers have associated such a larger step in admittance with poorer device performance. However, in this case, the exact opposite appears to be true.

Admittance spectra were then obtained over the same frequency ranges, but with an applied bias. Under reverse bias of 0.5 V, there were no changes in the spectra. The reduced Na sample spectra looked the same, and the magnitude of the step in the Na sample spectra changed in the manner expected for a bulk defect. The surprise came when the admittance spectra were obtained under forward bias. The reduced Na sample showed a clear activated step, while the higher Na sample showed only a hint of an additional step, as shown in Fig. 4(c) and (d).

For the admittance data shown in Fig. 5, we varied the forward bias while keeping the temperature constant. Here one sees the further development of this effect. In this case the reduced Na sample shows a very clear step between 180 K and 300 K, with an activation energy of 380 meV. The type of behavior exhibited in this figure clearly indicates the presence of large density of states near the interface for the reduced Na sample compared to the sample with higher Na. Specifically, the capacitance of the Na sample increases without any apparent bound as the forward bias is increased whereas, for the reduced Na sample, one appears to reach a limit near 35 nF/cm^2. This limit is indicative of a defect near the barrier interface that becomes more and more charged with increasing forward bias, thus limiting the collapse of the depletion region under forward bias. The fact that the step only appears under a limited range of bias also indicates that this defect is located in the interface.

The differing behavior under forward bias is by far the most profound difference between the Na and reduced Na samples, and so seems the most likely candidate to explain the difference in performance. Indeed, a sufficient large defect density in close proximity to the CdS/CIGS interface could easily affect the band bending and result in the 130mV observed difference in V_{oc}. If we assign this open circuit voltage loss exclusively to this defect, then by integrating Poisson's equation, we can estimate the amount of extra charge that is accumulating near the interface. Namely,

$$\Delta V = \frac{1}{\varepsilon}\int_0^\infty x\rho(x)dx \approx \frac{qN_{\text{int}}d}{\varepsilon}\ , \qquad (1)$$

where qN_{int} is the total sheet charge density present near the open circuit voltage condition, and d is the width of its spatial distribution from the barrier interface. For example, if we assume that d is 50 nm, then a 0.13 V difference in the device voltage requires a change of sheet charge density 1.6×10^{11} cm^{-2}.

We have also tried to reconcile this estimate with the results of our admittance and DLCP measurements discussed above. Figure 6 shows numerical calculations in which we place a deep defect of areal density near 10^{12} cm^{-2} within roughly 0.2 μm of the barrier interface, broadly distributed in energy. The change in its occupation over a change in bias equal to V_{OC} is then quite close to the above estimate. We see that it is then possible to closely reproduce both the observed drive-level profiles under forward bias exhibited by the reduced Na sample. We are currently pursuing further numerical modeling to attempt to also account in detail for both the admittance and cell performance behavior with such an assumed distribution of defect states near the barrier interface.

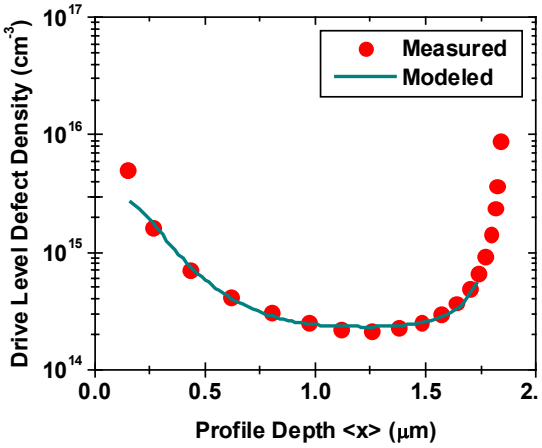

FIG. 6. Comparison of experimental reduced Na DLC profile (solid circles) with a calculation (line) based upon an assumed distribution of defects near the barrier interface.

REFERENCES

1. C. Lei, C.M. Li, A. Rockett and I.M. Robertson, J. Appl. Phys. **101**, 024909 (2007).
2. V. Lyahovitskaya, Y. Feldman, K. Gartsman, H. Cohen, C. Cytermann, and David Cahen, J. Appl. Phys., **91**, 4205 (2002).
3. A. Rockett, *Thin Solid Films* **480-1,** 2 (2005).
4. D. Rudmann, D. Bremaud, H. Zogg and A. N. Tiwari, J. Appl. Phys. **97**, 084903 (2005).
5. S.M. Wasim, C. Rincon, G. Marin, P. Bocaranda, E. Hernandez, I. Bonalde and E. Medina, Phys. Rev. B., **64**, 195101 (2001).